Hindawi
Complexity
Volume 2019, Article ID 1482051, 14 pages
https://doi.org/10.1155/2019/1482051

Research Article

A Study on the Dynamic Transmission Law of Spiral Drum Cutting Coal Rock Based on ANSYS/LS-DYNA Simulation

Lijuan Zhao,[1] Hongmei Liu ,[1] and Wenchao Zhou [2]

[1]*College of Mechanical Engineering, Liaoning Technical University, Fuxin 123000, China*
[2]*Baoding Railway Transformer Branch, China Railway Electric Industry Co. Ltd., Baoding 071051, China*

Correspondence should be addressed to Hongmei Liu; 56104170@qq.com and Wenchao Zhou; wenchao0726@163.com

Received 17 April 2018; Accepted 8 August 2018; Published 3 January 2019

Academic Editor: Mohamed Boutayeb

The ANSYS/LS-DYNA software has been used in this paper to establish the coal rock coupling model. A dynamic simulation of the cutting process was used to analyze the variation of the load. Based on the dynamic analysis of the coal and rock that were cut by the spiral drum, the stress cloud diagram of the coupled model of the spiral drum and the coal and the plastic domain evolution law of the coal and the rock were obtained from the coal to the rock. The time history curves of the parameters, such as the stress and strain of the drum and the pick, were obtained, and the stress distribution of the spiral drum during the working process was ascertained. The results showed that when the spiral drum cuts the interface between the coal and the rock, the coal and the rock collapsed and the working load fluctuated. Changing the traction speed in order to change the rotational speed of the drum had a more obvious effect on the load and the stress on the drum. Through the use of simulation, the stress distribution cloud diagram of the drum was obtained. The study has shown that the stress on the end plate was significantly higher than that on the cutting blade. The maximum stress acting on the alloy head was 1209.26 MPa. This study has provided a basis for the design and optimization of the drum with regard to reliability.

1. Introduction

The drum is the main working component of the shearer, and it acts to cut and load the coal. The load on the helical drum cutting coal, with a dirt band, is strong nonlinear, transient, and random. According to the literature [1], three kinds of tooth models with different structural shapes were established to study the stress distribution of the teeth with different structural shapes and rocks of different hardness using the LS-DYNA software. In the literature [2], LS-DYNA was used to simulate the process of the drum cutting the coal, and the load on the spiral drum was obtained under different cutting teeth arrangements. In the literature [3], LS-DYNA was used to simulate the cutting process of the drum, and the stress on the cutting teeth and the mass of the coal rock during the cutting process were analyzed. In the literature [4], LS-DYNA was used to simulate the cutting process of the drum that had four different structures, and the simulated load was added to the UG/NASTRAN software to predict the life span of the teeth. In the literature [5], LS-DYNA was used to simulate the truncated teeth cutting coal of different hardness, and the stress on the teeth was obtained. In the literature [6], the LS-DYNA software was used to simulate the load on the drum under different working conditions, the three-directional load and the load fluctuation coefficient of the drum were obtained, and the influence of the drum speed and traction speed on the load on the drum was analyzed. In the literature [7], the cutting part of the shearer in the process of cutting coal was simulated by LS-DYNA, and the load on the spiral drum was obtained, and the different motion parameters and the influence of cylinder stiffness on the reliability of the shearer's cutting component were analyzed. In the literature [8], the load curve of the drum was obtained through simulation of the cylinder cutting coal rock. The optimization design of the drum was carried out with the target of improving the cutting ratio energy consumption and the load fluctuation coefficient. In the literature [9], LS-DYNA was used to simulate the straight cutting and oblique cutting of the shearer, and the cutting resistance was smaller when the drum was cutting obliquely, and the weakest position of the drum was found. In the literature [10], LS-DYNA was used to simulate the new step drum cutting coal, and it was compared with the traditional shearer drum, and it was found that the cutting performance of the drum was better than that of the traditional shearer. However, the above studies did not consider the dynamic transmission problem of the cylinder drum cutting coal with a dirt band. Loui and Karanam [11] used finite element software to study the law of the tooth temperature change in 2005 and found the relationship between the surface temperature of the cutter, the speed of the drum, and the traction speed. In 2010, Gajewski and Jonak [12] carried out a cutting test of pick type and knife cut teeth of different wear states and obtained the cutting power and torque distribution law when cutting coal rock with different cutting teeth. Hoseinie et al. [13] analyzed the reliability of the key shearer system in 2012 and established the mathematical model of the reliability evaluation of the shearer. Taking the fault data of the shearer in an Iranian coal mine as the example, the reliability of each subsystem was modeled using the homogeneous Poisson process and the nonhomogeneous Poisson process, and the test was repeated. In 2013, Abu Bakar and Gertsch [14] carried out a cutting test on two types of coal and rock under both dry and wet conditions and obtained the axial cutting resistance and radial cutting resistance of the cutting teeth during the cutting of the rock. In 2014, Reid et al. [15] proposed a method of indirectly identifying the force dynamics of the cutting teeth by using the extended Kalman filter, and they verified the correctness of the method by numerical simulation. In 2016, Gospodarczyk [16] established a coal mining machine model of the coal breaking process according to the discrete element theory and analyzed the law of the coal flow movement change for the different motion parameters of different shearers.

In order to solve the dynamic transmission problems of the drum cutting coal rock, based on the finite element theory and broken coal, using PRO/E, the model of the spiral drum cutting coal containing a dirt band has been established by using ANSYS/LS-DYNA, and the LS-Prepost software simulated and obtained the dynamic transmission law of the spiral drum cutting coal containing a dirt band.

2. Establishment of the Finite Element Model of the Spiral Drum Cutting Coal with a Dirt Band

2.1. Establishment of the Three-Dimensional Solid Model of the Spiral Drum Cutting Coal with a Dirt Band. With the MG2*55/250-BWD thin coal mining machine drum as the research object and according to the design parameters of the drum's pick arrangement, as shown in Figure 1(a), a three-dimensional solid model of a shearer drum was built using the PRO/E software. PRO/E was used to establish a model of the coal rock and assemble with the drum. The drum and coal rock assembly model established in PRO/E was imported into ANSYS, and the three-dimensional model of the drum cutting coal has been shown in Figure 1(b).

2.2. Unit Type and Material Parameters and Finite Element Mesh Division. For the spiral drum and coal rock SOLID164 unit [17], the material of the tooth body was 42CrMo, and the alloy head material was YG8. The material of the square head, blade, end plate, and barrel body was 16Mn steel, and the material parameters of the spiral drum have been shown in Table 1.

In order to establish the simulated coal wall which conforms to the actual coal rock, physical and mechanical tests were required for the coal samples and dirt band samples, including density, compressive strength, elastic modulus, Poisson's ratio, cohesion, and internal friction angle. The test results have been shown in Table 2.

The square head was chosen to be *MAT_RIGID rigid material, and the other materials were selected as *MAT_ELASTIC elastic model. According to Table 1 and Table 2, the material parameters of the roller and the coal were set. Using solid164 to divide the coal rock and the drum, as shown in Figure 2, 695,586 units and 702,423 nodes were obtained.

2.3. Boundary Conditions and Constraints of the Model

2.3.1. Definition of Contact. The alloy head was defined as an erosion surface in contact with the coal rock [18], and the main slice was represented by the teeth, which was represented by the coal rock, as shown in Figure 3(a). The PART of the alloy head and the tooth body was used to define the contact CARDS with the coal and the rock. MSTYP was selected as 0 and the SOFT value was 1.

2.3.2. Defining the Boundary of the Coal Rock and the Constraints between the Model Parts. The coal rock was defined by the keyword *BOUNDARY_SPC_SET, as shown in Figure 3(b) (1, 3, 4) and was defined as having 6 degrees of freedom to prevent displacement. The keyword defining the unreflecting boundary condition was *BOUNDARY_NON_REFLECTING [19], as shown in Figure 3(b) (2, 5, 6, 7).

The barrel body, the teeth, the end plate, the alloy head, the blade, and the tooth base were set as the flexible body, and the square head was defined as the rigid body.

The connection between the rigid body and the flexible body needed to be defined as *CONSTRAINED_EXTRA_NODES; the connection between the flexible body and the flexible body was realized by using the conode method (extra nodes). The barrel body and the square head were rigidly coupled, and it was necessary to define the key *CONSTRAINED_EXTRA_NOEDES to connect certain nodes on the square head to the nodes on the barrel body. The keyword *EXTRA-NODES had a soft-soft connection between the tooth body and the tooth seat, as shown in Figure 3(c). The weld joints were defined between the alloy head and the tooth body using the keyword *CNSTRND_SPOTWELD, as shown in Figure 3(d).

2.3.3. Setting the Coal Rock Failure Parameters. The model of the coal and the rock was defined as *MAT-DRUCKE-PRAGER material; the material failure was set using the keyword *MAT_ADD_EROSION definition; the failure stress

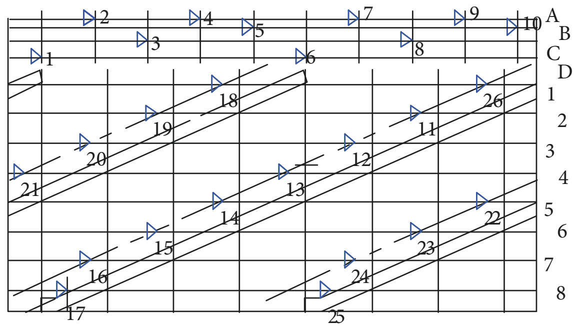

(a) Pick arrangement

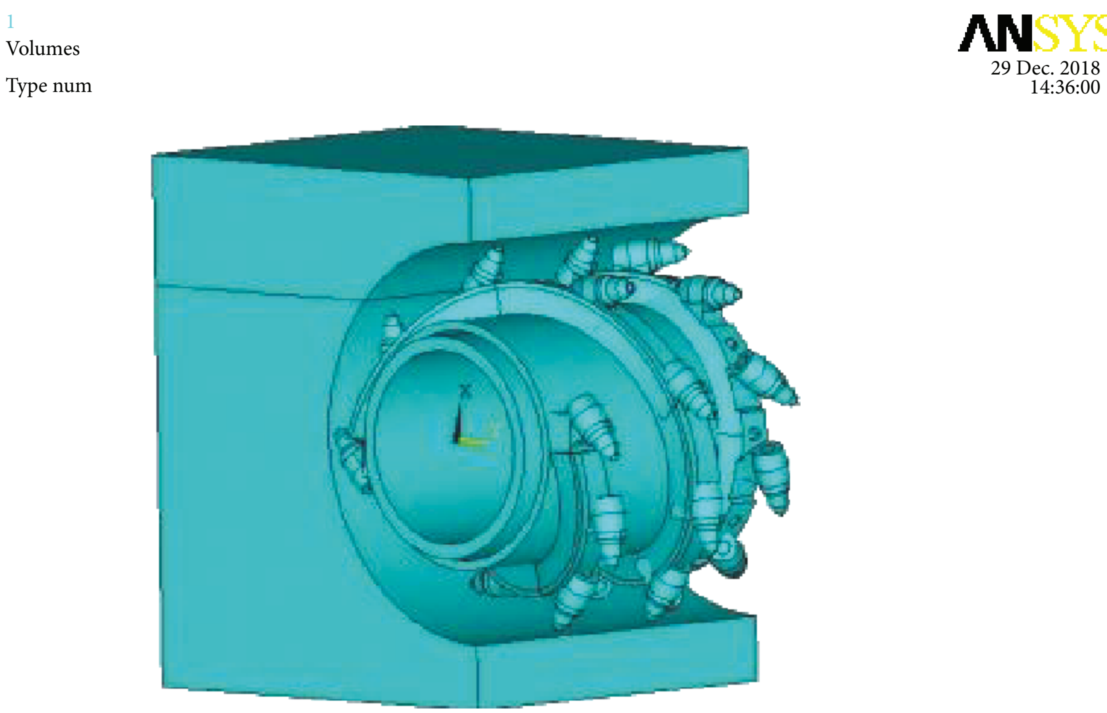

(b) Three-dimensional model of the drum cutting coal rock

Figure 1: The three-dimensional model of the drum cutting coal rock and the pick arrangement.

Table 1: Spiral drum material parameters.

Name	Density (kg/m^3)	Elastic modulus (MPa)	Poisson's ratio	Yield strength (MPa)	Tensile strength (MPa)
Alloy head	1.46e4	5.9e5	0.23	89 HRA	1500
Tooth body	7.85e3	2.125e5	0.3	1080	1200
Blade	7.85e3	2.187e5	0.3	766.67	862.03
Barrel body	7.85e3	2.187e5	0.3	766.67	862.03
End plate	7.85e3	2.187e5	0.3	766.67	862.03
Square head	7.85e3	2.187e5	0.3	766.67	862.03
Tooth base	7.85e3	2.187e5	0.3	766.67	862.03

of coal was set as 5.23 MPa; the failure stress of the dirt band was set as 52 MPa; the *CNSTRND_TIEBREAK keyword was used to define the failure of the coal and the dirt band.

2.3.4. Defining the Drive of the Spiral Drum, Solution Control, and Simulation. The coordinates of the mass center and the moment of inertia of the square head were calculated in Pro/E; the coordinates of the mass center and the moment of inertia were added to the keyword *PART_INERTIA. The curve of the drum speed was determined by *DEFINE_CURVE, and the traction speed was 4 m/min and the drum speed was 80 r/min. In order to analyze the

Table 2: The material parameters of coal and the dirt band.

Material	Density (kg/m^3)	Internal friction angle (°)	Cohesion (MPa)	Strength coefficient	Poisson's ratio	Elastic modulus (MPa)	Compressive strength (MPa)
Coal	1.32*e*3	58	1.45	1.9	0.23	4112	5.23
Rock	2.40*e*3	38	11.5	5.4	0.2	7670	52

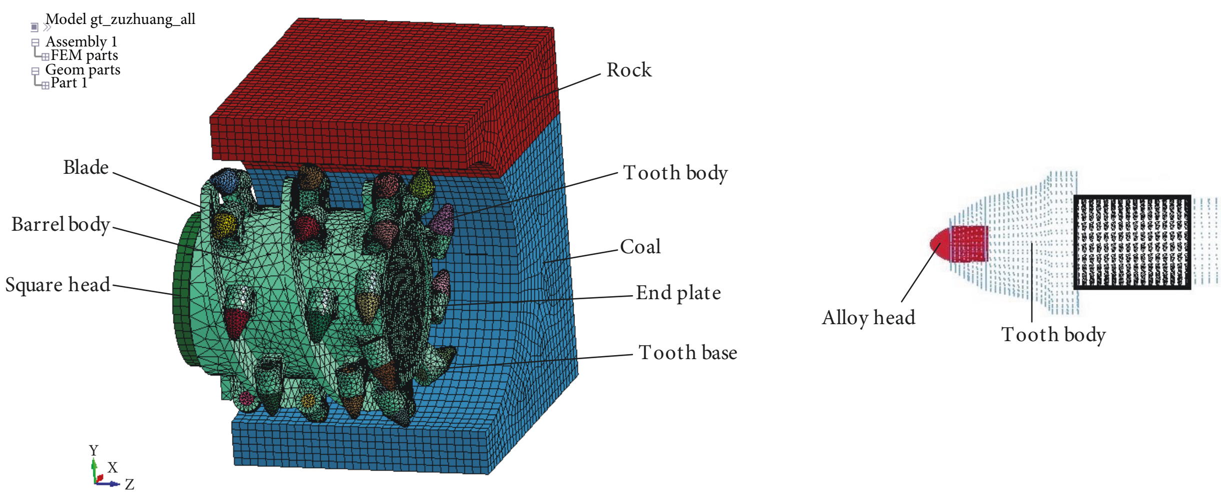

Figure 2: Finite element model of the roller and coal rock.

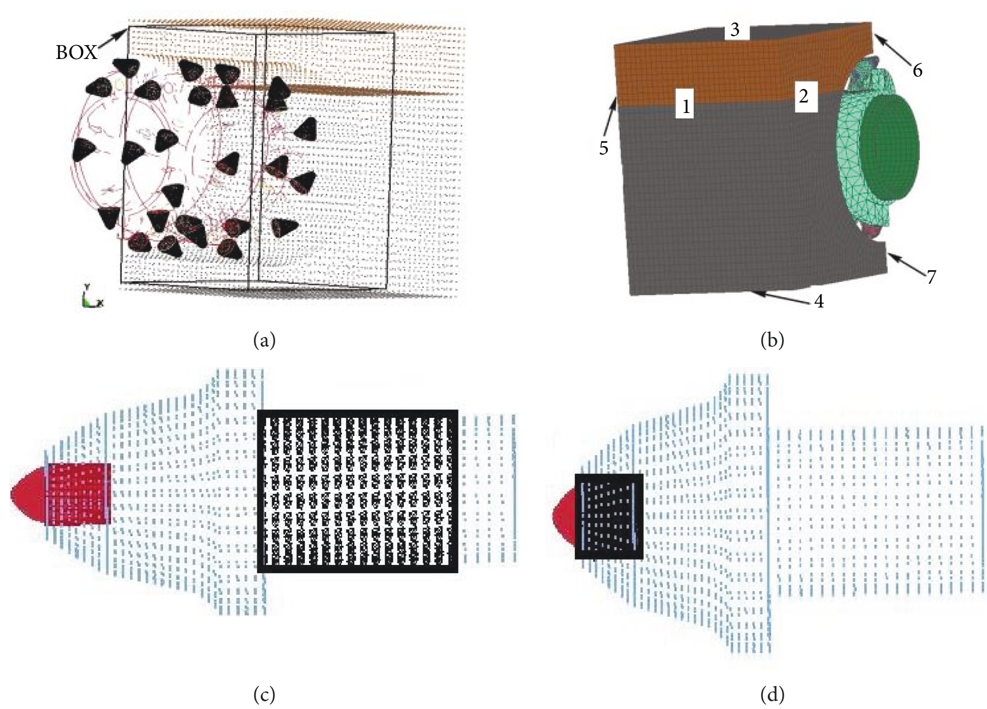

Figure 3: Boundary conditions and constraints of the model.

influence of the different motion parameters on the drum's dynamic transmission, 25 sets of different motion parameters were studied, namely, the traction speed was taken in 5 groups of 2 m/min, 3 m/min, 4 m/min, 5 m/min, and 6 m/min, respectively. The drum speed was set in 5 groups of 60 r/min, 70 r/min, 80 r/min, 90 r/min, and 100 r/min, respectively. The termination time *CONTROL_TERMINATION was set as 2 s. The energy control card defined the hourglass energy and the slip energy calculation, and the hourglass could be less than 10% of the total energy [20, 21], and 25 sets of working conditions were simulated, respectively.

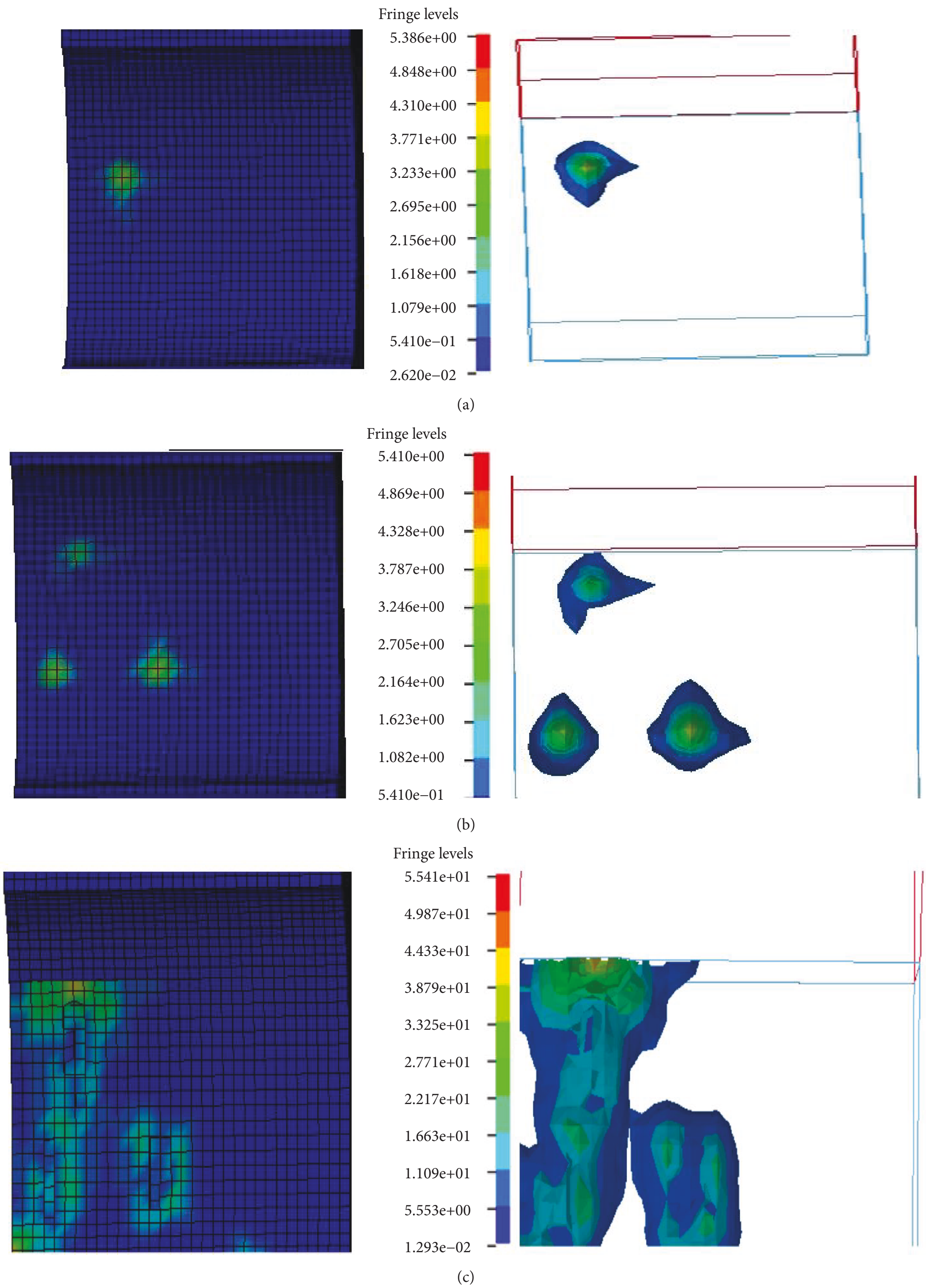

Figure 4: Continued.

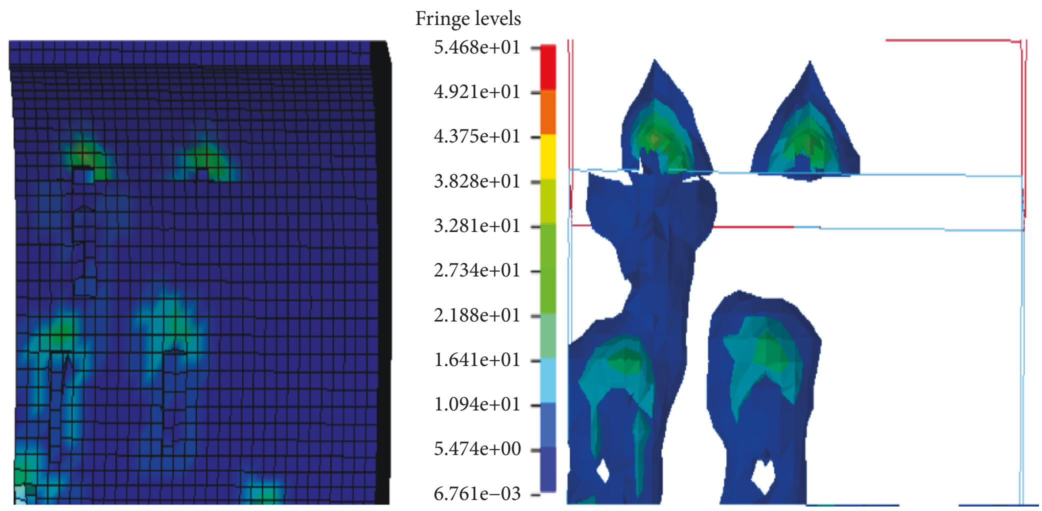

(d)

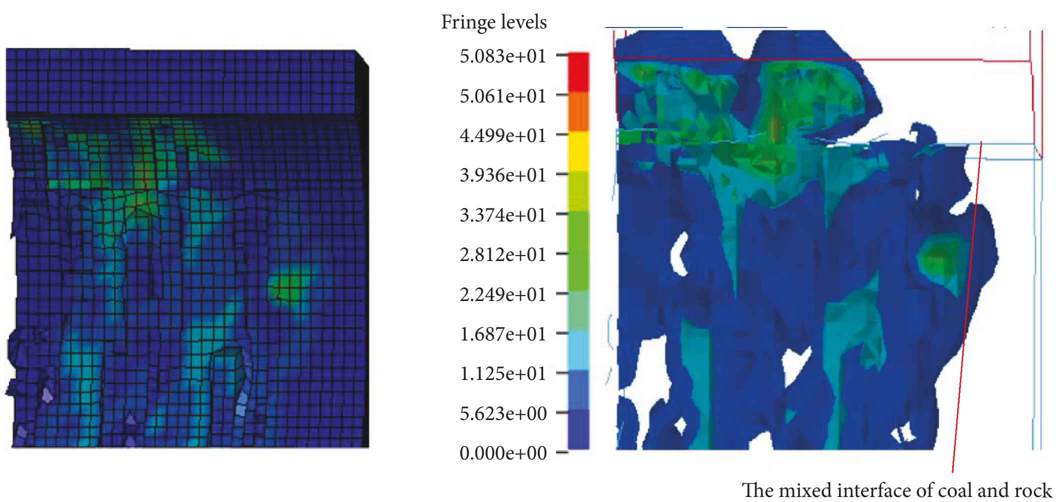

(e)

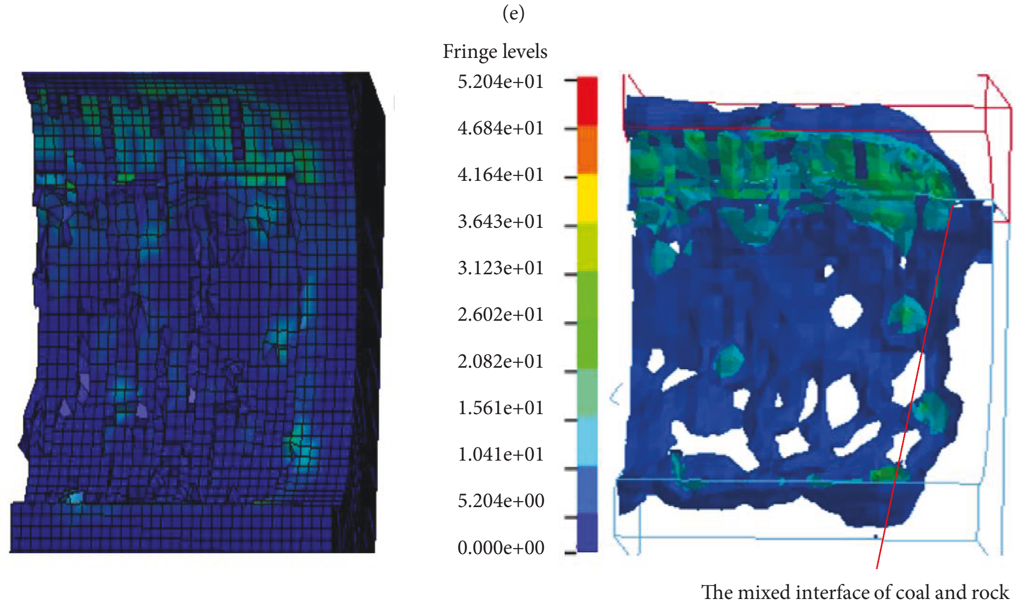

(f)

Figure 4: The process of the change of the coal and rock plastic region.

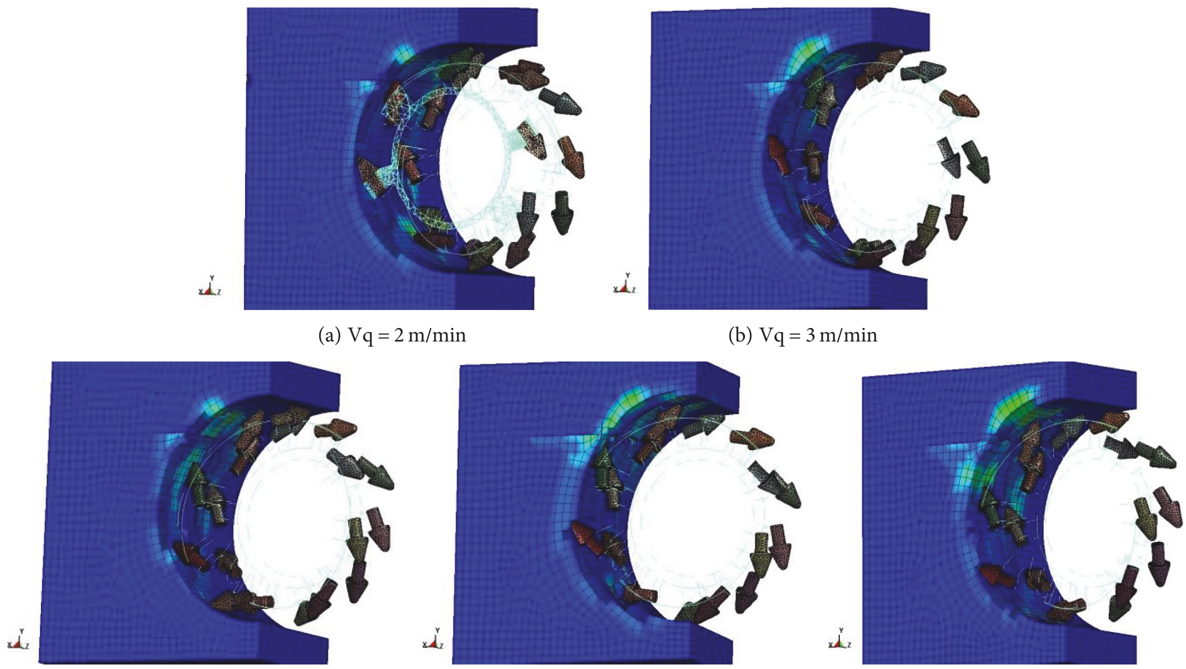

(a) Vq = 2 m/min (b) Vq = 3 m/min

(c) Vq = 4 m/min (d) Vq = 5 m/min (e) Vq = 6 m/min

Figure 5: Different traction speeds and coal rock stresses.

3. Analysis of the Simulation Results of the Spiral Drum Cutting Coal Rock

3.1. Analysis of the Plastic Deformation of the Coal Rock. In the posttreatment of the LS-DNA software, the plastic deformation of the coal rock was generated as shown in Figure 4. Figure 4 has shown the mixed interface of the coal rock, as shown in Figures 4(a)–4(f). From Figure 4(a), it can be seen that the drum rotates at first and there is only one cutting tooth in contact with the coal and the rock; coal and rock produced plastic deformation by cutting tooth extrusion; in Figure 4(a), the left side of the figure shows that there was only a tiny plastic domain, when the contact force reached its compressive strength; the local unit began to be crushed by coal damage, and at a stress of the coal of 5.2 MPa, the coal caved in. In Figure 4(b), it can be seen that there were three teeth in contact with the coal rock, and the plastic region of the coal rock was not continuous and was divided into three regions. It can be seen from Figure 4(c) that a cutting tooth on the blade just cuts to the mixture interface of coal and rock; the coal and rock stress was 55.4 MPa (the rock's compressive strength is 52 MPa) and the strain area was large; the unit in the coal rock mixing area near the broken caving occurred very obviously. It can be seen from Figure 4(d) that two teeth on the blade were involved in cutting the top rock. As the drum continued to cut, the contact area between the cutting teeth and the coal rock increased. It can be seen from Figure 4(e) that nearly 10 picks were involved in cutting the coal and rock; the plastic deformation area of the coal rock coupling was large, which shows that in addition to contact with the cutting teeth of the coal and rock unit damage, at the same time, the unit of coal and rock mixed area was partly destroyed. From Figure 4(f), it can be seen that the cutting was in a stable state, and the plastic region of the coal rock was continuously expanding and formed a zonal distribution and was filled with the inner surface of the coal rock model.

3.2. Influence of the Different Motion Parameters on the Dynamic Transmission of the Coal and Rock. The thickness of the chip will change if the matching speed between the drum and traction speed (Vq) is different, so that the stress area of the coal and rock will be affected. As shown in Figure 5, in the case of the same parameters, the greater the traction speed, the greater the area of stress in the coal and rock, and the greater the quality of the coal rock in the unit time, that is, the traction speed is proportional to the cutting efficiency.

In the case of the same parameters, the larger the rotational speed of the drum (n), the smaller the stress area of the coal and rock, which indicates that the cutting thickness was smaller, which leads to a decrease of the lump coal rate, as shown in Figure 6.

For different matching of the drum speed and traction speed, the relationship between the maximum stress value of the coal and rock and the movement parameters has been shown in Table 3 and Figure 7. In the cutting process, the difference between the drum speed and the traction speed directly affected the speed of the drum cutting coal rock and affected the stress of the coal and the rock. With the increase of the traction speed, the maximum stress value of the rock during cutting increased to varying degrees. When the traction speed was 2 m/min, 3 m/min, 4 m/min, 5 m/min, and 6 m/min, the speed of the spiral drum was 60 r/min, 70 r/min, 80 r/min, 90 r/min, and 100 r/min. The maximum rock stress increased by 6.497%, 7.175%, 9.280%, 8.164%, and 7.678%, respectively, and the amplitude

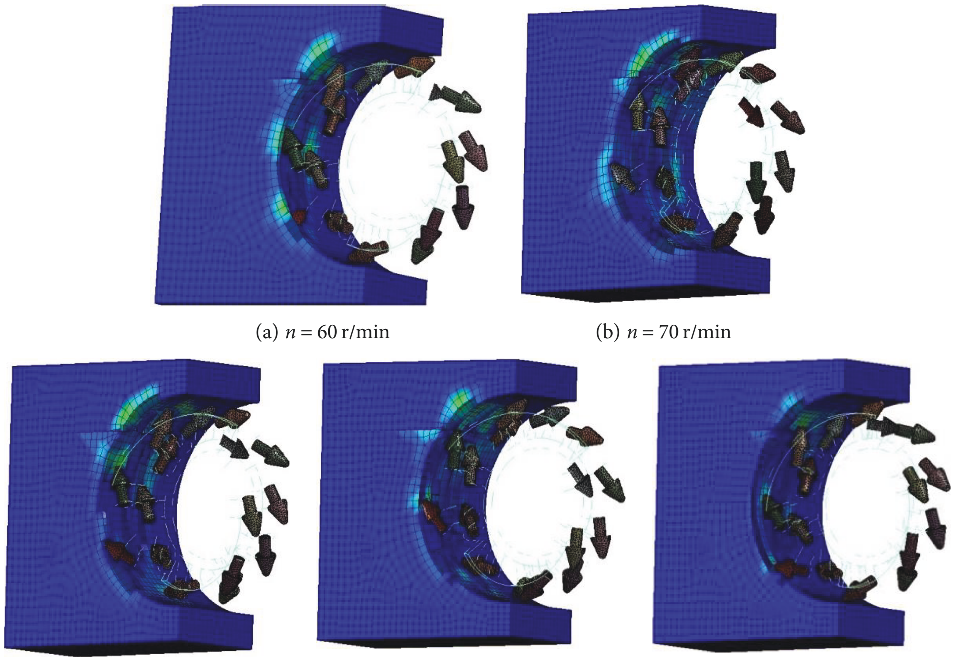

(a) $n = 60$ r/min (b) $n = 70$ r/min

(c) $n = 80$ r/min (d) $n = 90$ r/min (e) $n = 100$ r/min

Figure 6: Different drum speeds and the coal and rock stress.

Table 3: The statistical value of the rock stress (MPa).

Vq	n				
	60 r/min	70 r/min	80 r/min	90 r/min	100 r/min
2 m/min	55.78	54.91	53.12	52.67	51.96
3 m/min	57.51	56.28	55.34	54.38	53.17
4 m/min	59.03	58.37	57.53	56.75	55.39
5 m/min	59.32	58.54	57.57	57.12	56.76
6 m/min	59.46	58.85	58.05	56.97	55.95

increased first and then decreased gradually. The average stress increased by 7.778%. As the cutting speed increases and as the traction speed increases, the block size of the cut rock will also increase, which will cause the increase of the stress on the coal rock; the maximum stress of the rock during cutting occurred as the rotational speed of the drum increased. The values were reduced to different extents. When the rotating speed of the drum was 60 r/min, 70 r/min, 80 r/min, 90 r/min, and 100 r/min, the traction speed was 2 m/min, 3 m/min, 4 m/min, 5 m/min, and 6 m/min. The coal rock stress decreased by 7.744%, 7.546%, 6.166%, 4.315%, and 4.221%, and the decreasing amplitude gradually decreased, and the stress decreased by an average of 5.998%. This is due to the fact that when the drum's rotational speed increases, the pick cuts the coal rock, the acceleration increases, elastic energy and brittleness accumulate, but tenacity decreases, thereby resisting mutations in the force reduction. It can be seen that the influence of the change in traction speed on the rock stress during cutting was significantly greater than that of the drum speed.

As shown in Table 4 and Figure 7, with the increase of the traction speed, the maximum stress value of coal during cutting increased to varying degrees. When the traction speed was 2 m/min, 3 m/min, 4 m/min, 5 m/min, and 6 m/min, the spiral drum speed was 60 r/min, 80 r/min, 90 r/min, and 100 r/min. The maximum stress values of the coal increased by 29.37%, 34.44%, 40.12%, 32.54%, and 30.19%, respectively, and the amplitude increased first and then gradually decreased; the stress increased by an average of 33.332%. This is because when the traction speed increases, the cutting thickness also increases, the lump coal rate will increase which will cause the stress on the coal body to increase; as the rotation speed of the drum increases, the maximum stress value of the coal during cutting is reduced to varying degrees. When the drum speed was 60 r/min, 70 r/min, 80 r/min, 90 r/min, and 100 r/min, the traction speed was 2 m/min, 3 m/min, 4 m/min, 5 m/min, and 6 m/min. The maximum stress of the alloy head decreased by 17.07%, 27.00%, 26.31%, 20.24%, and 16.55%, respectively, and the decreasing amplitude first increased and then gradually decreased, and the stress was reduced by an average of 16.088%. The instantaneous speed of the teeth impacting on the coal rock is directly proportional to the impact velocity which will affect the expansion of internal cracks in the coal rock, resulting in the coal rock being truncated As the rotational speed of the drum increases, the acceleration of the cutoff coal body increases, the accumulated elastic energy and brittleness increase, but the toughness decreases, resulting in a decrease in the ability to resist mutation, and thus, the stress on the coal body is reduced.

4. Dynamic Analysis of the Drum

4.1. Extraction and Analysis of the Working Load of the Spiral Drum. The load of the spiral drum has been shown in

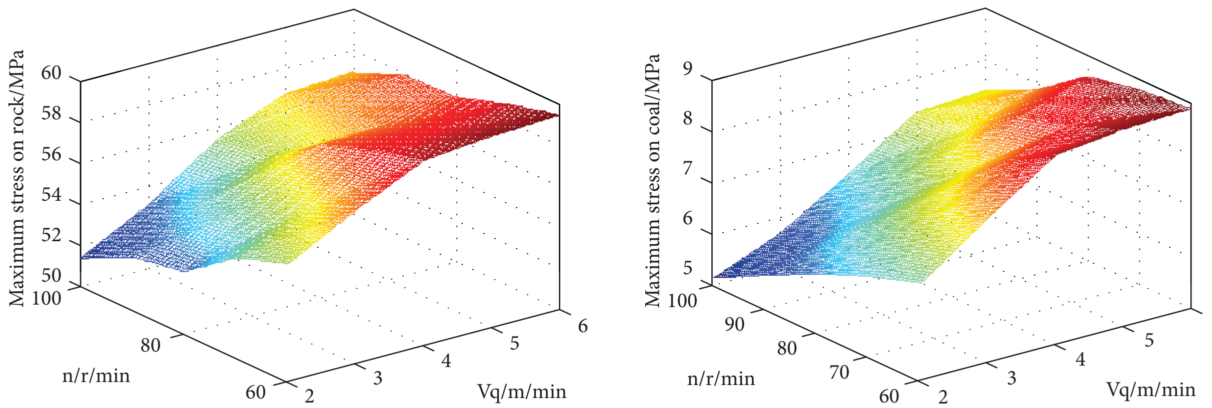

FIGURE 7: Relationship between the coal stress and the kinematic parameters.

TABLE 4: Statistical value of coal stress (MPa).

Vq	n			
	60 r/min	80 r/min	90 r/min	100 r/min
2 m/min	6.91	6.18	5.89	5.73
3 m/min	7.85	6.94	6.23	5.73
4 m/min	8.74	7.88	6.95	6.44
5 m/min	8.89	8.23	7.73	7.09
6 m/min	8.94	8.66	7.80	7.46

Figure 8 for when the drum speed was 80 r/min and the traction speed was 4 m/min. As shown in Figure 8(a), the total three-directional force of the drum increased as the number of teeth increased and the load was strong nonlinear, transient, and random. The three-directional force curve of the drum has been shown in Figure 8(b), from which it can be seen that the force in the Y direction was the largest, followed by the X direction, and the Z direction was the smallest. The Z direction force of the drum fluctuated above and below zero, but its average value was not zero. The X, Y, and Z directions are shown in Figure 2.

The results of the simulations of all the working conditions were sorted, as shown in Table 5. The average and load fluctuation coefficient of the three forces under the different working conditions of the 25 groups can be seen in Table 5.

In order to obtain the relationship between the roller motion parameters and the triaxial force under different working conditions, according to the Table 5 data, MATLAB was used to plot the motion parameters and the three-directional force diagram as shown in Figure 9. It can be seen from Figure 9 that, with the increase of the traction speed, the three forces that were both nonlinear increased, but the trend was different. Due to the increase of the traction speed, the cutting thickness of the truncated teeth in the unit time became larger, which increased the instantaneous load of the drum. With the increase of the degree of rotation, the nonlinearity decreased. When the rotating speed of the drum increased, the unit time of the drum to participate in the number of cutter teeth cutting was also increased, the same cutting line adjacent cutter teeth cutting time was shorter, and the corresponding cutting thickness would be smaller, so that the drum load was decreased. The occurrence condition of the thin coal seam was bad, the traction speed was generally low, and in order to guarantee a high loading rate, the drum speed was higher, but the coal's block degree was smaller, therefore producing a lot of coal dust. Therefore, it is necessary to make a reasonable match between the traction speed and the drum speed according to the occurrence condition of the coal seam.

4.2. Extraction and Analysis of the Working Load of the Pick Tooth. Obtaining the nonlinear load, when the picks pick up a complex coal seam, is very important for the design and use of the pick and even the shearer. Based on the simulation analysis, the working load of each cutting tooth on the spiral drum can be obtained, as shown in Figure 10, as the load spectrum of the resultant force on the intercepting teeth on the intercepting lines of the spiral drum.

4.3. Stress Analysis of the Drum. The stress cloud diagram of the drum when the traction speed was 4 m/min and the spiral speed of the drum was 80 r/min has been shown in Figure 11. From Figure 11(a), the stress of the 10th tooth body has been shown in Figure 11(b). Figure 11(b) has shown that the stress the tooth body suffered was below 1000 MPa, which is less than its yield strength. Among them, 149,559 units on the axles of the head of the tooth body were subjected to the maximum stress, with a maximum value of 812.5 MPa. Figure 11(c) has shown the stress of the alloy head of no. 11. Figure 11(c) has shown that the alloy head tooth space affected by stress was significantly larger than the former blade on both sides, there was a large range, and the maximum stress was 1209.26 MPa, within the scope of the materials needed. The stress distribution of the blade, barrel body, and tooth has been shown in Figure 11(d), which has shown that stress was mainly concentrated at the root of the tooth base. In addition, the stress on the tooth base on the end plate was greater than that of the blade. The maximum stress at the root of the tooth base was 371.79 MPa.

5. Conclusion

(1) Based on the ANSYS/LS-DYNA software, the model of the spiral drum cutting coal containing a dirt band was established and a dynamic simulation of the

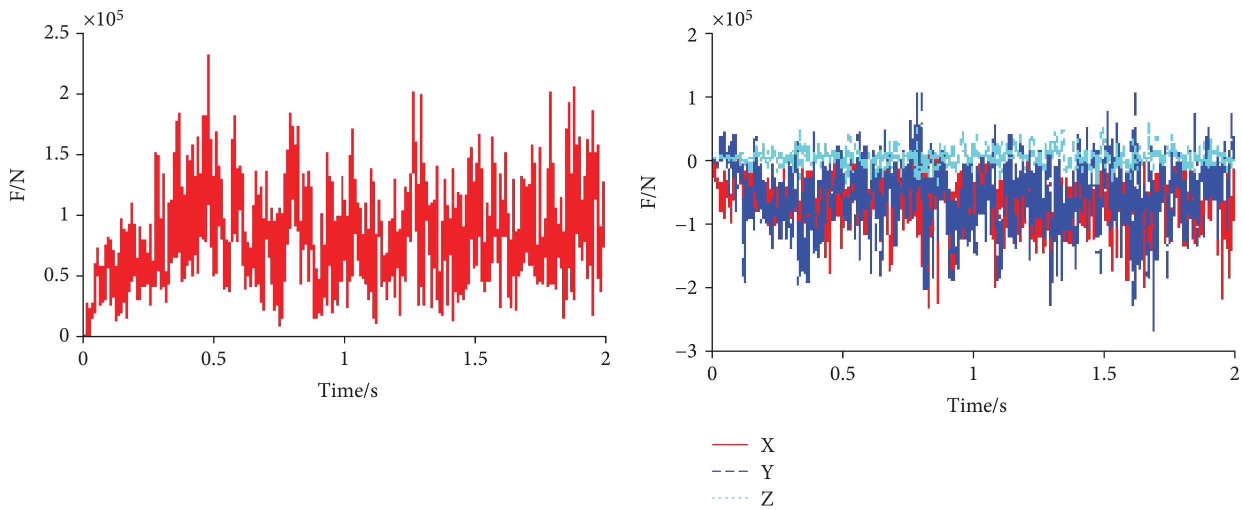

(a) The total force of the drum

(b) The triaxial force of the drum

Figure 8: The force of the spiral drum.

Table 5: Simulation results of the drum's triaxial force.

Traction speed (m/min)	Rotational speed (r/min)	X force mean (N)	Fluctuation coefficient of X force	Y force mean (N)	Fluctuation coefficient of Y force	Z force mean (N)	Fluctuation coefficient of Z force
2	60	2.30e4	0.3674	3.13e4	0.7435	6.21e3	0.0964
2	70	3.18e4	0.3312	3.98e4	0.7061	7.56e3	0.0931
2	80	3.73e4	0.3163	4.61e4	0.6819	8.92e3	0.0923
2	90	4.10e4	0.3012	5.15e4	0.6693	9.82e3	0.0918
2	100	4.41e4	0.2894	5.51e4	0.6637	1.05e4	0.0912
3	60	2.23e4	0.3502	2.91e4	0.7248	6.15e3	0.0959
3	70	2.95e4	0.3241	3.69e4	0.6826	7.92e3	0.0925
3	80	3.37e4	0.3096	4.21e4	0.6614	8.27e3	0.0912
3	90	3.76e4	0.2903	4.70e4	0.6477	9.35e3	0.0904
3	100	4.20e4	0.2786	5.05e4	0.6401	1.04e4	0.0896
4	60	2.05e4	0.3397	2.66e4	0.7043	5.44e3	0.0946
4	70	2.71e4	0.3101	3.39e4	0.6637	6.77e3	0.0905
4	80	3.21e4	0.2934	4.01e4	0.6481	7.53e3	0.0896
4	90	3.63e4	0.2805	4.34e4	0.6352	8.39e3	0.0882
4	100	3.83e4	0.2697	4.55e4	0.6298	9.13e3	0.0873
5	60	1.85e4	0.3203	2.42e4	0.6864	5.00e3	0.0931
5	70	2.43e4	0.2914	3.04e4	0.6427	6.29e3	0.0896
5	80	2.99e4	0.2746	3.74e4	0.6219	7.03e3	0.0878
5	90	3.30e4	0.2623	3.91e4	0.6126	7.98e3	0.0864
5	100	3.62e4	0.2497	4.10e4	0.6057	8.36e3	0.0857
6	60	1.66e4	0.2868	2.19e4	0.6637	4.78e3	0.0919
6	70	2.28e4	0.2517	2.76e4	0.6204	5.76e3	0.0876
6	80	2.67e4	0.2349	3.15e4	0.5993	6.82e3	0.0854
6	90	2.90e4	0.2274	3.50e4	0.5845	7.45e3	0.0843
6	100	3.42e4	0.2199	3.70e4	0.5776	7.95e3	0.0836

cutting process was carried out, and the drum load was obtained for several different working conditions. Through analysis of the coal and rock plastic domain, it was found that when the cutting teeth cut into the dirt band, the stress on the coal and cutter tooth will produce mutation, and obvious fracture and caving will appear near the mixture of the coal and rock interface unit

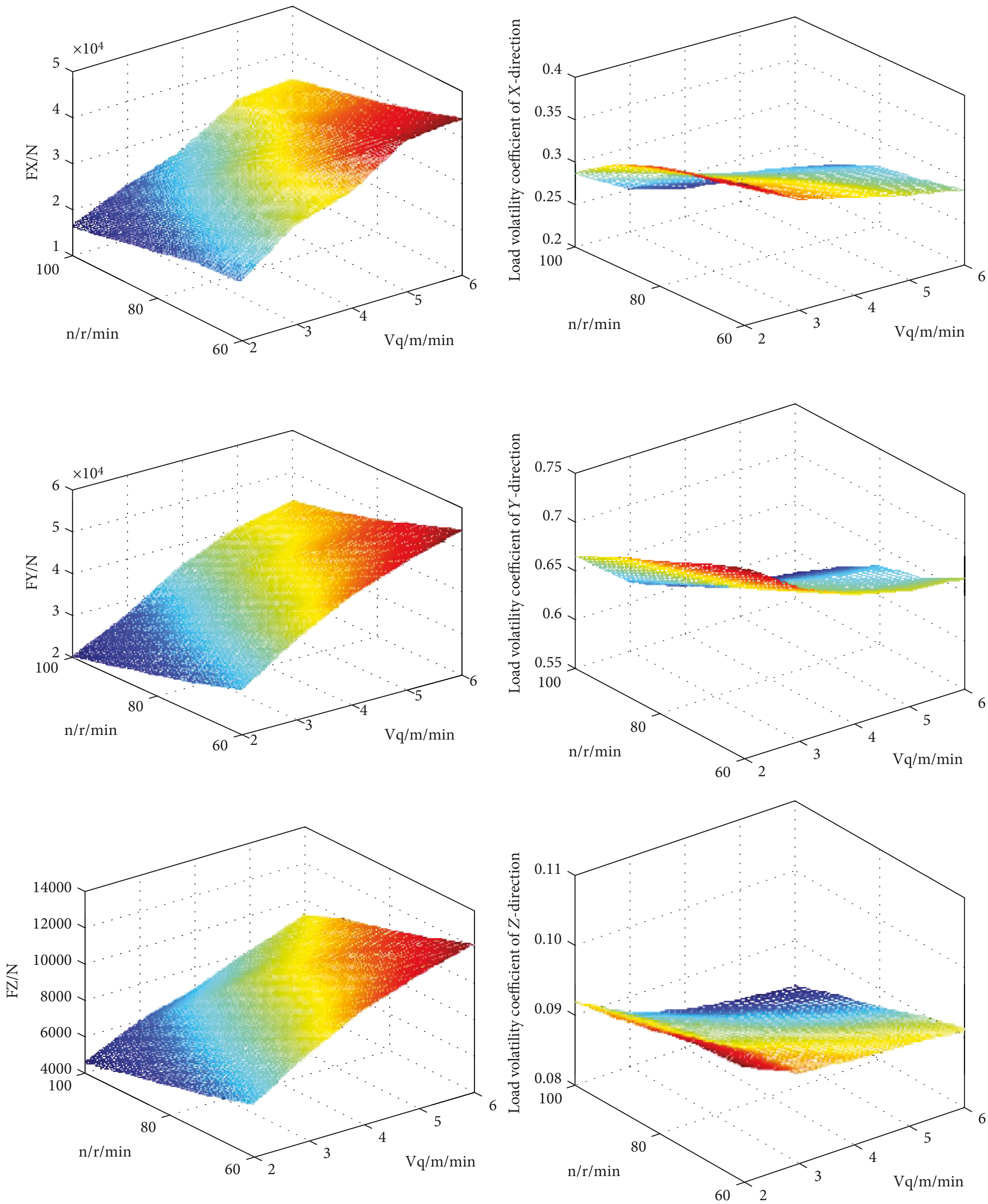

Figure 9: Relation between the motion parameters and the triaxial force of the drum.

(2) By analyzing the variation law of the three-way force acting on the drum, it was found that the three-directional force of the drum increased with the increase of the traction speed and the increase was smaller and smaller when the rotational speed of the drum was constant. When the traction speed increased from 2 m/min to 6 m/min, the force in the X direction increased by an average of 87.49%, the

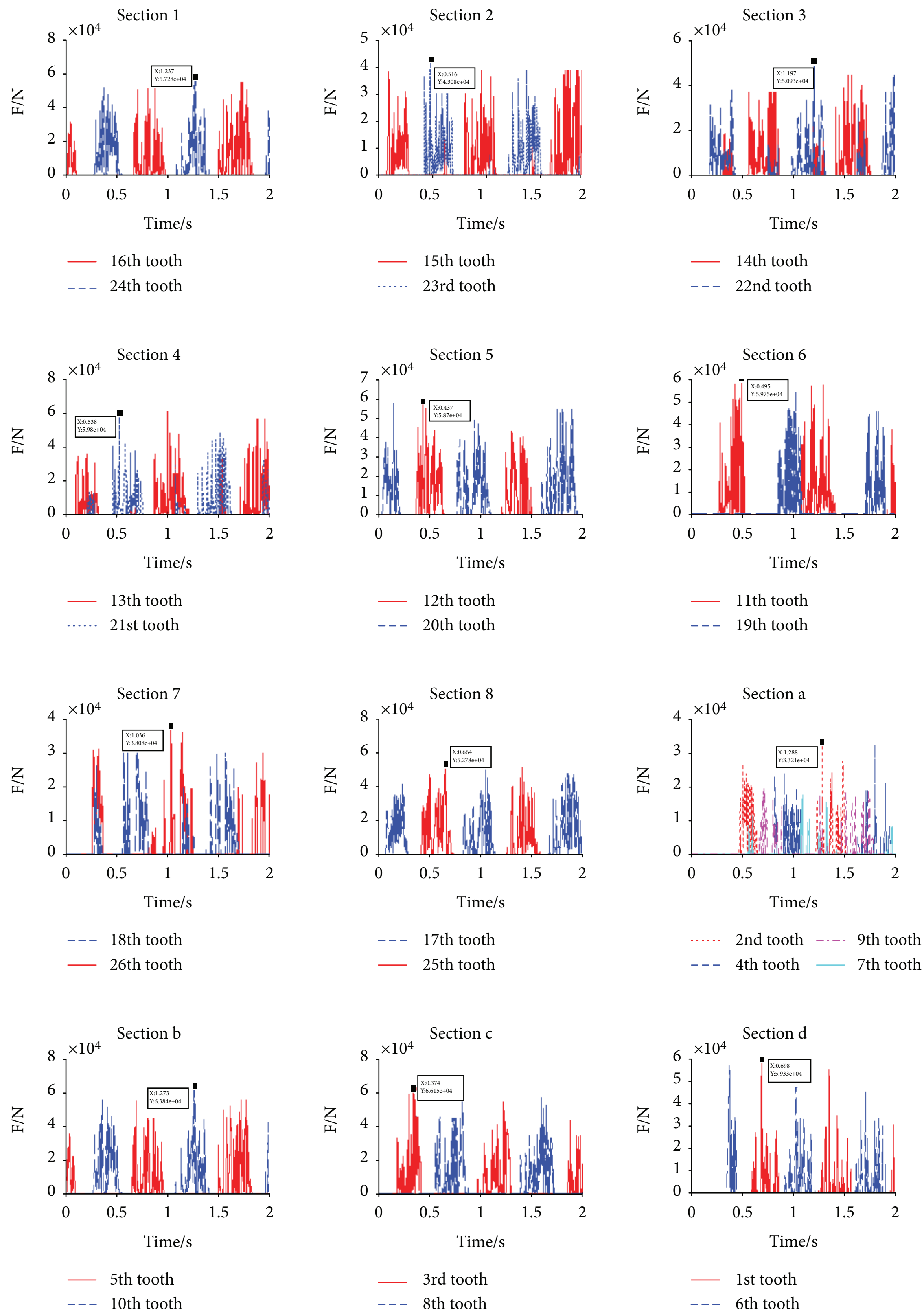

FIGURE 10: The cutting force.

force in the Y direction increased by an average of 71.80%, the force in the Z direction increased by an average of 67.74%, and the change of the traction speed had the greatest influence on the force in the X direction. The force in the Y direction was the next highest, and the force in the Z direction was the

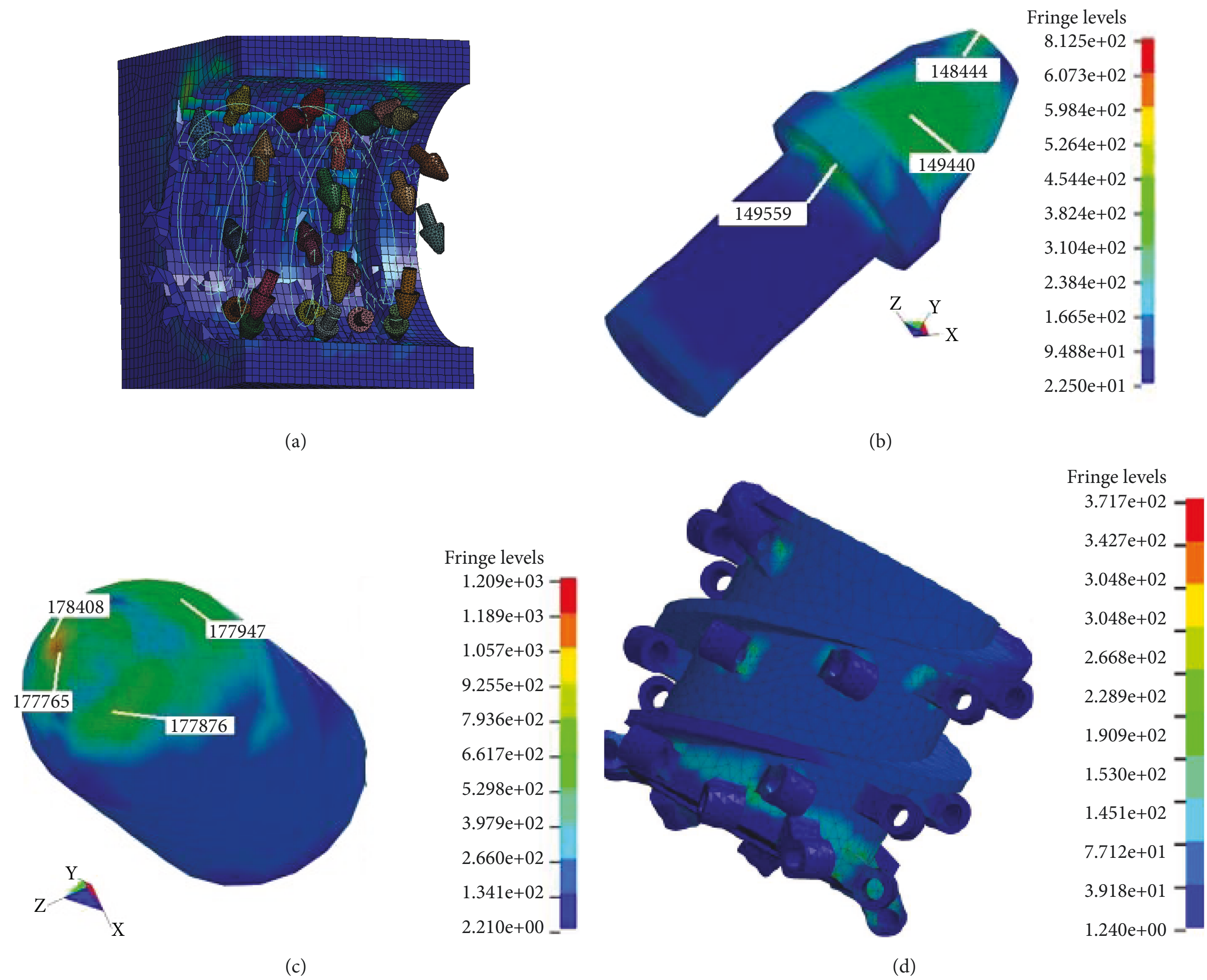

Figure 11: Stress cloud diagram of the drum and teeth.

smallest. For the same traction speed, the three-directional force of the drum decreased with the increase of the rotational speed of the drum, the force in the X direction decreased by an average of 28.83%, and the force in the Y direction decreased by an average of 31.44%, the force in the Z direction was reduced by an average of 23.75%, and the influence of the traction speed and the rotational speed of the drum on the three-way force of the drum was analyzed and compared. It was found that the influence of the traction speed on the load was much greater than that of the drum's rotational speed

(3) By analyzing the different motion parameters obtained from the simulation, the stress changes of the lower coal rock body were analyzed. It was found that under the same conditions of the other parameters, the stress region affected by the coal rock increased with the increase of the traction speed and decreased with the increase of the rotational speed of the drum. When the rotating speed of the drum was the same, when the pulling speed was increased from 2 m/min to 6 m/min, the increase in the stress of the coal rock first increased and then gradually decreased, and the stress values of the rock and coal were increased by 7.778% and 33.332%, respectively. When the pulling speed was the same, and when the rotating speed of the drum was increased from 60 r/min to 100 r/min, the stress reduction of the coal rock was gradually reduced, and the stress values of the rock and the coal body were reduced by 5.998% and 16.088%, respectively. In comparison, it was found that the influence of the change of the motion parameters on the stress of the coal body was obviously greater than the stress of the rock

(4) Through simulation, the stress distribution cloud diagram of the drum was obtained for a traction speed of 4 m/min and a rotation speed of 80 r/min. The study showed that the stress on the end plate was significantly higher than that on the blade. The maximum stress of the drum mainly focused on the local contact area of the tooth tip of the alloy head

and the axial shoulder of the tooth body head. The maximum stress of the alloy head was 1209.26 MPa, and the maximum stress of the tooth body was 812.5 MPa. The stress of the truncated teeth was mainly concentrated at the root of the tooth base, and the maximum stress was 371.79 MPa

Data Availability

The data used to support the findings of this study are available from the corresponding author upon request.

Conflicts of Interest

The authors declare that they have no conflicts of interest.

Acknowledgments

The study was supported by the National Natural Science Foundation of China (51674134) and the Liaoning Provincial Department of Education (LJ2017QL017).

References

[1] Y. An, "Simulation analysis on strength of cutting picks with various shapes based on LS-DYNA," *Coal Mine Machinery*, vol. 39, no. 12, pp. 5–8, 2011.

[2] J. He and Z. Wang, "Numerical simulation of the process of spiral drum cutting coal in thin coal seam," *Coal Engineering*, vol. 45, no. 6, pp. 97–99, 2013.

[3] R. Dong, *Study on Numerical Simulation of the Spiral Drum Cutting Coal Rock*, Liaoning Technology University, 2012.

[4] H. Lu, Y. Zhu, and Y. Wang, "Analysis and optimization for pick line distance of shearer roller," *Journal of Taiyuan University of Technology*, vol. 5, pp. 584–588, 2013.

[5] T. Wu, "Research on the strength of the cutting teeth of the excavator based on ls-dyna under different hardness of coal," *Mechanical Engineer*, vol. 12, pp. 171-172, 2013.

[6] J. Xue, L. Zhao, and Y. Liang, "Analysis of shearer drum motion parameters based on LS-DYNA," *Coal Mine Machinery*, vol. 6, pp. 81–83, 2014.

[7] H. Guo, *Research on Dynamic Characteristics of Drum Shearer Cutting Unit*, China university of mining and technology, 2014.

[8] Q. Wu, *Structural Parameters Optimization for Cutting Drum of Coal Cutting Machine*, Taiyuan University of Technology, 2015.

[9] Z. Song, Z. Yuan, and Z. Hao, "Numerical simulation of cutting coal of shearer drum based on ANSYSLS-DYNA," *Shanxi Coal*, vol. 36, no. 2, pp. 1–4, 2016.

[10] F. Zhou and S. Liu, "Research on the cutting performance of ladder drum," *Coal Engineering*, vol. 49, no. 2, pp. 128–130, 2017.

[11] J. P. Loui and U. M. R. Karanam, "Heat transfer simulation in drag–pick cutting of rocks," *Tunnelling and Underground Space Technology*, vol. 20, no. 3, pp. 263–270, 2005.

[12] J. Gajewski and J. Jonak, "Towards the identification of worn picks on cutterdrums based on torque and power signals using artificial neural networks," *Tunnelling and Underground Space Technology*, vol. 26, no. 1, pp. 22–28, 2011.

[13] S. Hadi Hoseinie, M. Ataei, R. Khalokakaie, B. Ghodrati, and U. Kumar, "Reliability analysis of drum shearer machine at mechanized longwall mines," *Journal of Quality in Maintenance Engineering*, vol. 18, no. 1, pp. 98–119, 2012.

[14] M. Z. A. Bakar and L. S. Gertsch, "Evaluation of saturation effects on drag pick cutting of a brittle sandstone from full scale linear cutting tests," *Tunnelling and Underground Space Technology*, vol. 34, no. 1, pp. 124–134, 2013.

[15] A. W. Reid, P. R. McAree, P. A. Meehan, and H. Gurgenci, "Longwall shearer cutting force estimation," *Journal of Dynamic Systems, Measurement, and Control*, vol. 136, no. 3, article 031008, 2014.

[16] P. Gospodarczyk, "Modeling and simulation of coal loading by cutting drum in flat seams," *Archives of Mining Sciences*, vol. 61, no. 2, pp. 365–379, 2016.

[17] W. A. N. G. Li, G. A. O. Xiaofeng, and J. I. A. O. Li, "Simulation and analysis for helical drum cutting coal rock by LS-DYNA," *Coal Mine Machinery*, vol. 34, no. 12, pp. 41–44, 2013.

[18] Z. Liming and X. Jin, "Simulation study of theory of cutting for shearer drum author institution," *Coal Mine Machinery*, vol. 34, no. 10, pp. 44-45, 2013.

[19] Z. Weiguo, L. Zenglu, and G. Tong, "Impact characteristics of picks under different working conditions," *Journal of Liaoning Technical University (Natural Science)*, vol. 33, no. 9, pp. 1279–1283, 2014.

[20] W. Zhengrong, X. Xiaoyan, and Z. Hong, "Study on conical pick cutting using LS-DYNA," *Journal of Vibration, Measurement & Diagnosis*, vol. 30, no. 2, pp. 163–165, 2010.

[21] N. Gunes Yilmaz, M. Yurdakul, and R. M. Goktan, "Prediction of radial bit cutting force in high-strength rocks using multiple linear regression analysis," *International Journal of Rock Mechanics & Mining Sciences*, vol. 44, pp. 960–970, 2007.